Vietnam Journal of Earth Sciences, 47(3), 411–429, https://doi.org/10.15625/2615-9783/23431

Vietnam Journal of Earth Sciences

https://vjs.ac.vn/index.php/jse

Performance evaluation of RegCM5 in long-term convection-permitting simulations for high-urbanized areas in Vietnam

Thanh Nguyen-Xuan*, Dzung Nguyen-Le, Thanh Ngo-Duc

Department of Space and Earth Sciences, University of Science and Technology of Hanoi (USTH), Vietnam Academy of Science and Technology (VAST), Hanoi, Vietnam

Received 24 June 2025; Received in revised form 26 August 2025; Accepted 11 September 2025

ABSTRACT

This study is the first in Vietnam to assess the impact of urbanization on the local climate in Hanoi and Ho Chi Minh City using the Regional Climate Model version 5 (RegCM5) at convection-permitting (CP) resolution. Simulations were conducted at a horizontal grid spacing of 2 km, driven by the fifth-generation global reanalysis produced by the European Centre for Medium-Range Weather Forecasts (ERA5), and incorporating annually updated urban information from 2000 to 2020. Unlike previous studies that relied on coarse-resolution simulations and static urban data, the latest version of RegCM5 enables stable long-term simulations with significantly reduced computational demands. The results yield three key findings. First, the 2 km simulations outperform those at 10 km resolution, highlighting the advantages of CP-scale modeling. In specific cases, the 2 km simulations even surpass the performance of the Vietnam Gridded Climate (VnGC) dataset when validated against station observations. Second, incorporating updated urban information allows the model to more accurately capture the temporal evolution of urbanization impacts, particularly evident from late afternoon (around 16:00 local solar time, LST) to midnight (around 01:00 LST). Third, the study finds that the urban heat island (UHI) effect in both cities is stronger during this late afternoon to midnight period and intensifies with increasing background temperatures. The UHI magnitude in Hanoi is generally greater than in Ho Chi Minh City.

Keywords: Convection Permitting, RegCM5, Urban modeling.

1. Introduction

Urbanization has emerged as one of the most significant anthropogenic processes influencing regional climate, particularly in developing countries undergoing rapid economic growth (United Nations, 2018). Vietnam, with its accelerated urban expansion over recent decades, presents an exemplary case for examining the climatic consequences of urbanization, especially in densely populated areas such as Hanoi and Ho Chi Minh City. The transformation of natural land surfaces into urban infrastructures not only alters land-atmosphere interactions but also intensifies urban heat island (UHI) effects, modifies meteorological patterns, and contributes to the occurrence of extreme weather events (Grimmond et al., 2009; Qian et al., 2022). Notably, while urban expansion may exacerbate the adverse effects of extreme heatwaves in regions where heat stress has frequently surpassed dangerous levels during

*Corresponding author, Email: nguyen-xuan.thanh@usth.edu.vn

summer, recent studies in Vietnam indicate that the country is projected to experience substantial increases in heat stress in the future (Nguyen-Le et al., 2025).

Dynamical downscaling through regional climate models (RCMs) is crucial for accurately representing climate at local to regional scales and is a prerequisite for assessing the climate impacts of urbanization. The complexity of urban environments necessitates high-resolution models that can capture land-atmosphere interactions at both mesoscale and metropolitan scales. The Regional Climate Model (RegCM), developed in 1989 at the Abdus Salam International Centre for Theoretical Physics (ICTP) (Giorgi et al., 1990), has been extensively used both globally and in Vietnam for regional climate simulations (e.g., Nguyen-Thi et al., 2019; Hoang-Cong et al., 2022; Nguyen-Ngoc-Bich et al., 2022; Ngo-Duc et al., 2024) and benefits from strong community support (Giorgi et al., 2019). The latest version, RegCM5, integrates the MOLOCH dynamical core (Davolio et al., 2020), offering notable improvements in both simulation accuracy and computational efficiency (Giorgi et al., 2023). However, due to its novelty, the application of RegCM5 at convection-permitting (CP) scales using a horizontal grid spacing of ~2–4 km to resolve convective processes and better capture fine-scale urban effects explicitly remains limited. This gap is particularly pronounced in tropical monsoon regions such as Vietnam, where mesoscale dynamics and rapid land-use change interact in complex and nonlinear ways.

Initial experiments employing RegCM5 with the MOLOCH dynamical core have demonstrated superior performance compared to previous versions, including both RegCM4 and RegCM5 with the older dynamics, across various statistical metrics and computational efficiency criteria (Giorgi et al., 2023). The newly developed model system enhances the capability to simulate at CP resolutions. It supports stable integrations with time steps up to five times longer than in previous versions, leading to significant gains in computational efficiency (Giorgi et al., 2023). This improvement is essential for the climate modeling community, especially in developing countries like Vietnam, where computational resources are limited, precisely the target users for whom RegCM was designed initially (Pal et al., 2007). In a recent study, Nguyen-Xuan et al. (2025) conducted the first performance evaluation of RegCM5 for Vietnam, showing that the model, when using the new dynamical core at a 10 km horizontal resolution, outperforms its predecessors. The study also employed a Micro Genetic Algorithm to identify the optimal configuration of physical parameters for simulations over Vietnam at this resolution. These promising findings have motivated further applications of RegCM5, particularly for investigating finer-scale processes in urban areas.

Within this context, the present study aims to explore the potential of applying RegCM5 for downscaling at a 2 km CP resolution over Vietnam. The primary objective is to assess the long-term climate impacts of urbanization in Hanoi and Ho Chi Minh City, two rapidly expanding megacities. Unlike previous studies that employed coarser resolutions or static representations of urban land cover, this study performs a high-resolution (2 km) RegCM5 simulation, driven by reanalysis data and annually updated urban land cover over the recent 20-year period (2000–2020). Model performance is evaluated against in-situ station observations and an observational-based gridded dataset, with particular attention to temperature patterns, diurnal UHI variation, and sensitivity to background warming. The findings will provide valuable insights for urban policy development and climate adaptation planning in Vietnam,

particularly in areas such as disaster prevention, flood risk assessment, and public health management.

2. Experimental Design

2.1. Domain and Model Settings

The RegCM5 model is configured to simulate across three domains, with their designs and topographic characteristics illustrated in Fig. 1. The experiments span 21 years from 2000 to 2020. Each year, the model runs from May 1st to August 31st, with the analysis focusing on the summer months (June, July, and August-JJA), while the May simulation serves as spin-up time.

The first domain (D1) (Fig. 1a), commonly referred to as the "mother domain", is designed with a longitude-latitude dimension of 201 × 245 grid points and 18 vertical pressure levels ranging from 1000 mb to 5 mb, simulating at a horizontal resolution of 10 × 10 km. The central area of this domain encompasses the entire territory of Vietnam. Simulations for D1 use initial and boundary conditions (ICBC) from ERA5 the fifth-generation global reanalysis produced by the European Centre for Medium-Range Weather Forecasts (ECMWF) (Hersbach et al., 2020). The results from the D1 simulations are simultaneously further downscaled to two subdomains focusing on Hanoi (D2-HN) (Fig. 1b) and Ho Chi Minh City (D2-HCM) (Fig. 1c). Both subdomains are designed for CP simulations with a horizontal resolution of 2 × 2 km, a longitude-latitude dimension of 112 × 112 grid points, and 44 vertical pressure levels. Figures 1b and 1c also indicate that both cities are located in large, flat delta regions: the Red River delta for Hanoi and the Mekong River delta for Ho Chi Minh City.

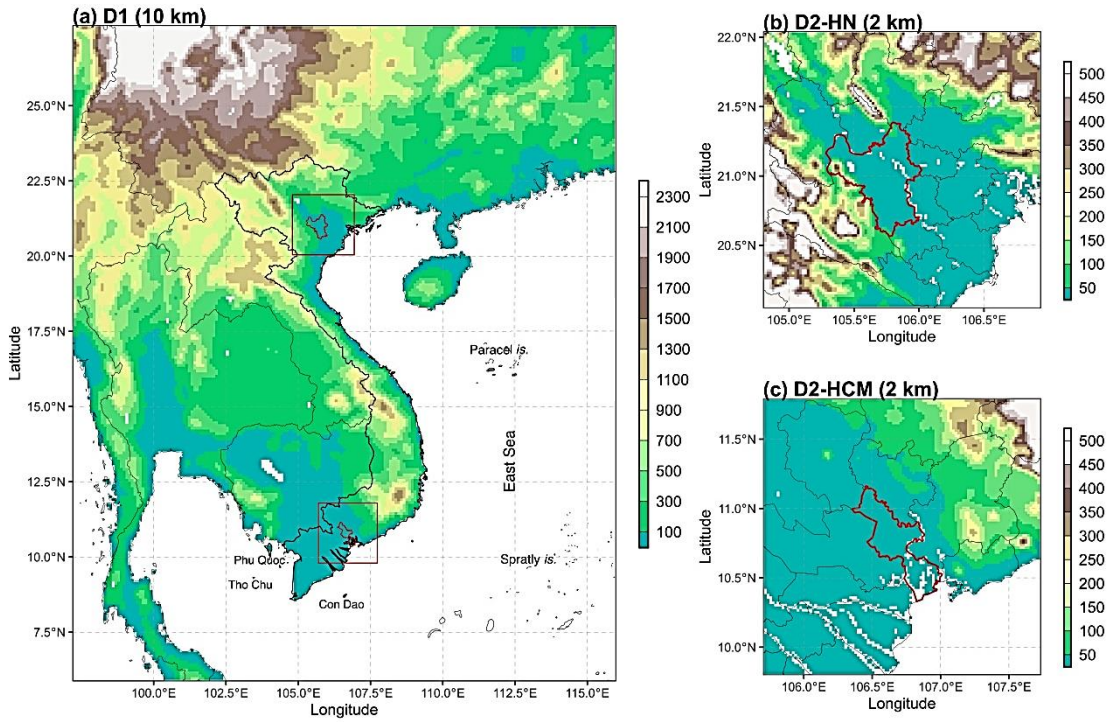

Figure 1. Domains and topography characteristics, including (a) Domain 1 (D1), with a horizontal resolution of 10 km; (b) subdomain D2-HN focusing on Hanoi; and (c) subdomain D2-HCM focusing on Ho Chi Minh City. Both D2-HN and D2-HCM have a horizontal resolution of 2 km. Topographic data are obtained from the Shuttle Radar Topography Mission (NASA SRTM, 2013)

Regarding the physical parameterization settings, Table 1 summarizes the key configurations applied to the three domains. Specifically, the setup for the D1 simulations follows that used in our previous study (Nguyen-Xuan et al., 2025), in which the Micro-Genetic Algorithm was applied to identify the optimal physical parameterization configuration for RegCM5 over an identical domain. Although this configuration was initially designed to optimize model performance for precipitation, it also performed well in representing temperature, outperforming other configurations across all metrics. Therefore, at the time of this study, we considered it the most suitable choice for simulating temperature over the domain, and additional sensitivity tests were not carried out. In brief, the main configurations for D1 include the MOLOCH dynamics core (Coppola et al., 2021), the Community Land Model version 4.5 (CLM4.5) for land surface processes (Oleson et al., 2013), the Zeng ocean flux scheme with the roughness option 2 (Zeng et al., 1998), and the NCAR CCM3 radiation scheme (Kiehl et al., 1998). Convective parameterization schemes (CPS) employ the Tiedtke scheme over land (Tiedtke, 1989) and the Emanuel scheme over the ocean (Emanuel, 1991). Microphysics parameterizations (MP) use the Subgrid Explicit Moisture Scheme (SUBEX) (Pal et al., 2000), while the Holtslag scheme (Holtslag et al., 1990) is adopted for planetary boundary layer (PBL) processes. Lateral boundary conditions are handled using a relaxation-exponential technique.

Table 1. Summary of the experimental design employed in this study using RegCM5. "Default" refers to experiments using fixed LULC throughout the study period (2000–2020), while "Urban" refers to those incorporating annually updated LULC data.

Domain name	**Experiment**	**Dimensions** (Lon×Lat×Lev)	**Grid size**	**Configurations**		
				CPS	**MPS**	**Shared configurations**
D1	Default	201 × 245 × 18	10 km	Tiedtke over land and Emanuel over the ocean	SUBEX	Dynamics: MOLOCH Land surface model: CLM4.5 Ocean flux scheme: Zeng-2 Radiation: CCM3 PBL: Holtslag Lateral boundary conditions
D2-HN-Def	Default	112 × 112 × 44	2 km	Off	Nogherotto-Tompkins	
D2-HN-Urb	Urban					
D2-HCM-Def	Default					
D2-HCM-Urb	Urban					

For the two D2 simulations, most configurations are maintained as in D1, except that the CP is disabled and the MP is replaced with the ICTP Nogherotto-Tompkins (Nogherotto et al., 2016) due to its relatively better performance demonstrated in a recent study of RegCM5 at CP scale (Giorgi et al., 2023). To evaluate the impacts of rapid urbanization in the two cities, we conduct two experiments for each. The first experiment (denoted as "Default") utilizes fixed land-use and land-cover (LULC) information provided within CLM4.5 throughout the 21 years, while the second experiment (denoted as "Urban") incorporates annually updated LULC data over the same period. More detailed information on the LULC data is provided in Section 2.2.

2.2. Data and Processing

To evaluate the model outputs, we collected and processed four different types of datasets, including:

(1) ERA5 reanalysis: The European Centre for Medium-Range Weather Forecasts (ECMWF), reanalysis version 5 (ERA5,

Hersbach et al., 2020) was collected for the period 2000–2020 and used as the initial and boundary conditions for downscaling over the D1 domain.

(2) Annually updated LULC data: The global time-series maps of population count at 1-km spatial resolution (Gao and O'Neill, 2020) were utilized to analyze population trends, thereby enabling the annual update of LULC information in the D2-HN and D2-HCM subdomains for the period 2000–2020. The dataset provides population information for each 1 × 1 km grid point at 10-year intervals for the base year 2000 and the future period until 2100 under five Shared Socioeconomic Pathways (SSPs). A preliminary analysis (Supplementary Fig. S1) reveals significant population growth from 2000 to 2020, with a pronounced concentration in the cities' centers. While the differences among the five SSP scenarios for 2000, 2010, and 2020 are minimal (Supplementary Fig. 1d), we chose the scenario with the highest expansion rate, anticipating that it will amplify the model's representation of urban effects. Accordingly, we opted for SSP5 to derive population changes in the two subdomains.

The fixed LULC data used in RegCM5, derived from CLM4.5 (Jackson et al., 2010) and updated by Oleson and Feddema (2019), aligns with the 2010 population data from Gao and O'Neill (2020). In CLM4.5, LULC is represented using a mosaic approach, in which urban areas are defined as fractions (percentages) of each grid cell and categorized into medium, high, and very high density (e.g., tall building districts). To estimate urbanization trends before and after 2010, annual relative population changes derived from the SSP5 data discussed above were used to adjust the fractions of urban categories. It should be noted that although this method may not fully capture the complexity of real-world urbanization processes in the Hanoi and Ho Chi Minh City domains, it provides a valuable basis for exploring the potential impacts of urbanization on the local climate.

(3) Gridded observational temperature data: Daily mean 2-m temperature data from the Vietnam Gridded Climate Dataset (VnGC) (Trinh-Tuan et al., 2019) are used to validate the RegCM5 simulations. The VnGC provides daily fields at a horizontal resolution of 10 × 10 km for the period 2000–2018.

(4) Station data: Temperature data from several stations in the Hanoi and Ho Chi Minh City regions were collected to perform in-depth validations of the RegCM5 simulations. Figure S2 illustrates the location of the stations along with the estimated data availability (in percent) during the 2000–2020 period. While the Hanoi domain includes many stations with high data availability, the Ho Chi Minh City domain lacks a sufficient number of stations, and the available data for each station in and around Ho Chi Minh City is relatively low. Consequently, the analysis using station data will focus on the Hanoi domain.

It's worth noting that, compared to "Default" experiments that use only urban land recorded in 2010, the "Urban" experiments use annually updated data based on population changes. This approach raises concerns about how urban characteristics within a grid point can change with population density shifts. However, this can be resolved within the urban canopy model used in our simulation, commonly known as CLMU, which is a part of the Community Land Model version 4.5 (CLM4.5). CLMU employs a mosaic approach, where each grid point can encompass the fractions of three urban density types (UDTs), each associated with distinct characteristics (e.g., building heights, properties of walls, roofs, roads, pre-set parameters for estimating anthropogenic heat fluxes, etc.). As we modify urban land

use, the fractions of the three UDTs also change, leading to changes in their energy fluxes that result in a total flux change. Although using population-based information may make the experiment less realistic, the changes in the total flux of the urban updating experiment not only reflect changes in urban morphology but, more importantly, also reflect changes in anthropogenic fluxes due to population changes.

2.3. Method for Estimating the Urban Heat Island (UHI) Effect

The Urban Heat Island (UHI) effect is a crucial indicator for characterizing urban climate. Typically, UHI is defined as the temperature difference between urban and rural areas (urban minus rural), which is the most widely recognized approach (Nguyen-Xuan and Im, 2023). The intensity of UHI depends on the choice of surrounding rural areas as a reference (Martin-Vide et al., 2015; Yan et al., 2016). Consequently, we adopt a method similar to that proposed by Nguyen-Xuan and Im (2023), which uses inverse distance weighting (IDW; Shepard, 1968) to estimate the temperature difference between each urban grid point and its neighboring lower-density urban grid points, rather than limiting the reference to predefined rural grid points. Specifically, for each urban grid point *"i"*, the UHI_i is computed as follows:

$$UHI_i = \frac{\sum_{r=1}^{r=n}\left[\frac{\left(T_{adjusted,i} - T_{adjusted,r}\right)}{\left(D_{ir}^2\right)}\right]}{\sum_{r=1}^{r=n}\left[\frac{1}{\left(D_{ir}^2\right)}\right]} \quad (1)$$

In Equation (1), temperatures are first adjusted for elevation at each grid point. This adjustment is necessary because urban grid points are generally located below 100 m. In contrast, rural grid points are sometimes at higher elevations, which may lead to an overestimation of UHI intensity based on raw temperature differences. To address this, temperatures are adjusted using an average lapse rate of 0.65°C per 100 m, consistent with previous studies (Lowry, 1977; Martin-Vide et al., 2015; Ünal et al., 2020). In the equation, *n* denotes the number of neighboring lower-density grid points (*r)*, and *D* represents the distance (in kilometers) from the urban grid point *i* to each *r*.

3. Results

3.1. Daily 2-m Temperature at Different Resolutions

Simulated 2-m temperatures for the period 2000–2018, obtained from the RegCM5 D1 and D2 experiments at 10 km and 2 km resolutions, respectively, are compared against observational data from in-situ stations, the gridded VnGC data, and ERA5 reanalysis data (Fig. 2). Overall, RegCM5 simulations demonstrate improvements over ERA5 data, with higher resolution providing more detailed information.

In the Hanoi region, ERA5 shows a cold bias compared to VnGC. The D1 simulation, at 10 km resolution, exhibits a warm bias. Meanwhile, in the Ho Chi Minh City region, both ERA5 and the 10 km D1 experiment show a cold bias relative to VnGC. At the same resolution, the temperature distributions simulated by the D1 experiments are pretty similar to those derived from VnGC, particularly for the Hanoi domain. For both cities, the D2 experiments at 2 km resolution clearly show distinct warm biases compared to VnGC.

When incorporating station observations, significant differences in signals and conclusions are observed. The VnGC data appears to smooth temperature values at station locations, resulting in an underestimation of high temperatures at urbanized stations like Hanoi, and an overestimation of low temperatures at mountainous stations such as TamDao. This discrepancy is due to the limited number of stations used to construct VnGC and the smoothing effect of the interpolation technique.

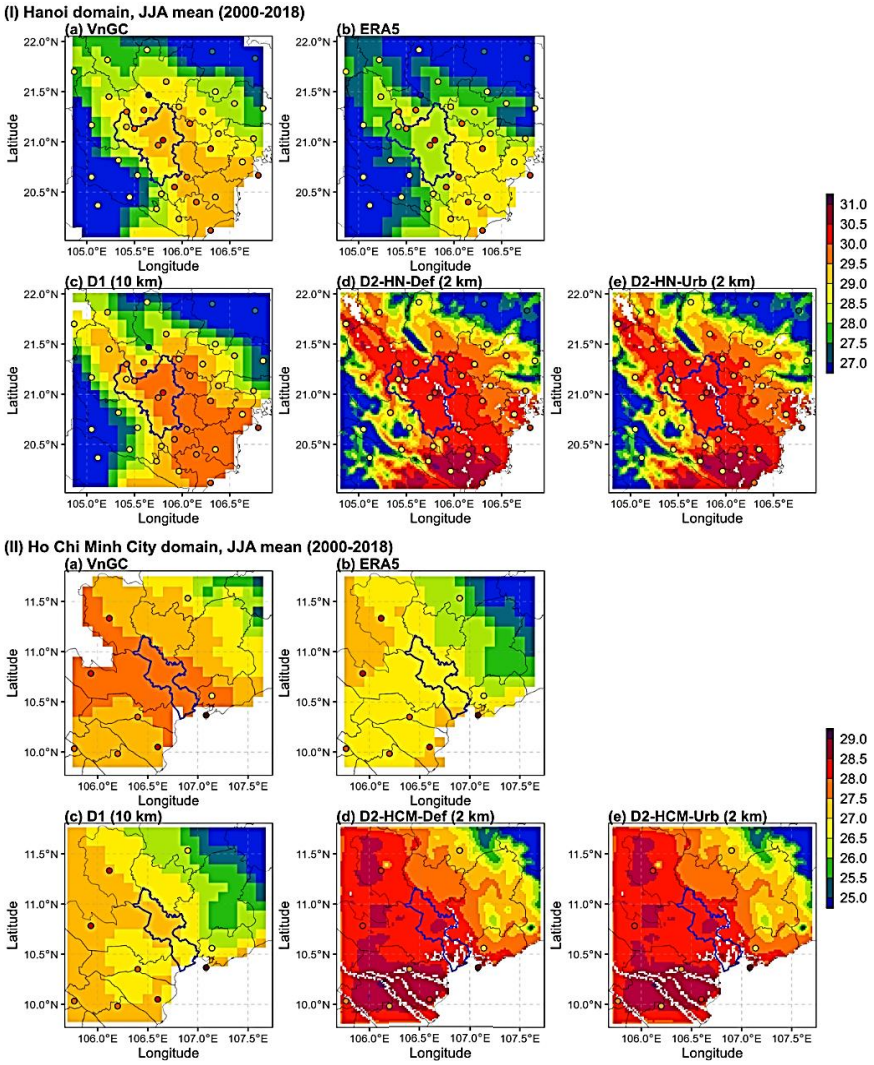

Figure 2. Climatological mean (2000–2018) of JJA 2-m temperature (unit: °C) from (a) VnGC, (b) ERA5, (c) the D1 experiment, (d) the D2 experiment with default CLM4.5 urban data, and (e) the D2 experiment with annually updated urban data. Observations from in-situ stations are shown as filled circles. Panels (I) and (II) correspond to the Hanoi and the Ho Chi Minh domains, respectively.

The CP downscaling experiments at 2 km resolution align more closely with station observations compared to the D1 simulations at 10 km resolution, which tend to underestimate station temperatures. For each city, both 2 km simulations, the default and the updated urban cases, display somewhat similar climatological patterns. This similarity can be explained by the fact that the updated urban case is characterized by lower urbanization during the first 10 years and increased urbanization during the last 10 years, compared to the constant 2010 data in the default case. This temporal change in the updated urban case results in lower temperatures at the beginning and higher temperatures toward the end, leading to similar average values over the entire period.

It is noteworthy that the RegCM5 experiments may exhibit systematic biases, as they inherit the configuration optimized by Nguyen-Xuan et al. (2025) for simulating

precipitation at a 10 km resolution. Consequently, their capability to simulate temperature may require further adjustment. However, the results depicted in Fig. 2 show that higher resolution enables the capture of more detailed processes. For instance, simulations at 2 km resolution reveal relatively warmer areas in the center of the two cities and relatively colder areas in the surrounding rural regions. This highlights both the advantages and the necessity of performing dynamical downscaling at the CP scale.

Figure 3 displays the comparison at highly urbanized station locations, i.e., stations located at grid points with an urban percentage in 2010 greater than or equal to 15%. Due to the lack of highly urbanized station data in the Ho Chi Minh City region, the analysis is limited to the Hanoi region. Overall, the RegCM5 simulations show improvements compared to the ERA5 reanalysis, with higher-resolution experiments yielding better performance. Although there are some differences between the two CP scale simulations, particularly noticeable in the early years and toward the end of the study period, both outperform the 10 km resolution simulation.

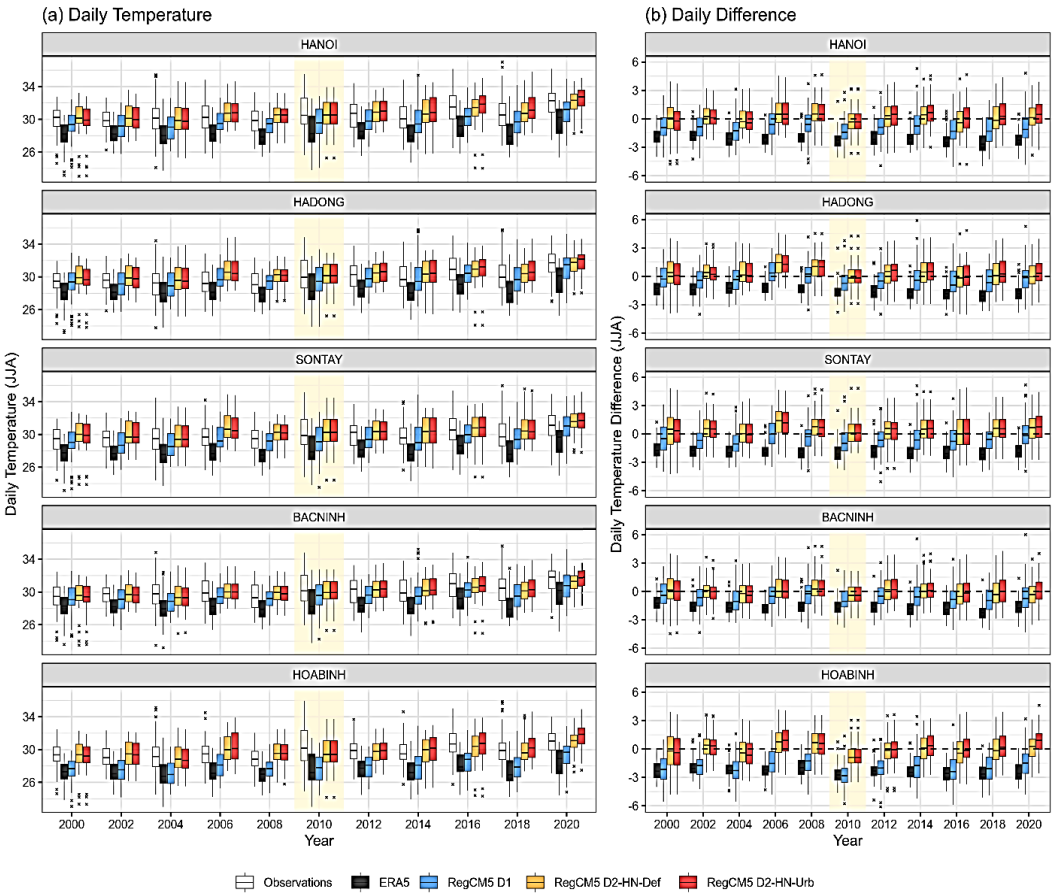

Figure 3. Boxplots at specific highly urbanized stations in the Hanoi domain for yearly comparison of: (a) daily 2-m temperature (unit: °C) from observations, ERA5, the D1 experiment, the D2-HN-Def experiment, and the D2-HN-Urb experiment; and (b) daily differences (unit: °C) between model outputs and observations. The year 2010 is highlighted with yellow shading to indicate when both D2 experiments used the same urban information

This is evident in the biases shown in Fig. 3b: ERA5 and the 10 km RegCM5 simulation underestimate temperatures at highly urbanized stations, while the two CP-scale experiments exhibit smaller biases that are symmetrically distributed around zero. In rural areas (Fig. 3S), RegCM5 also generally demonstrates improved performance at higher resolutions, although the pattern is not uniform. For example, at TamDao, a relatively high-altitude station, both ERA5 and the 10 km RegCM5 simulation significantly overestimate temperature, whereas the two 2 km experiments reduce this bias. The statistical metrics shown in Table 2 further support these findings.

Table 2. Summary of statistical metrics for ERA5, RegCM5 simulations, and observations at different urban and non-urban stations

	Station name	**Metrics**	**ERA5**	**RegCM5 D1**	**RegCM5 D2-HN-Def**	**RegCM5 D2-HN-Urb**
Urban	HANOI	ME	-2.119	-0.847	0.264	0.343
		RMSE	2.319	1.717	1.540	1.551
	HADONG	ME	-1.540	-0.181	0.490	0.484
		RMSE	1.793	1.499	1.553	1.514
	SONTAY	ME	-1.879	-0.396	0.609	0.569
		RMSE	2.092	1.605	1.642	1.630
	BACNINH	ME	-1.679	-0.515	0.039	0.088
		RMSE	1.912	1.511	1.416	1.417
	HOABINH	ME	-2.236	-1.773	0.189	0.313
		RMSE	2.427	2.307	1.562	1.618
Non-Urban	BAVI	ME	-1.346	-0.110	0.918	0.892
		RMSE	1.615	1.593	1.806	1.792
	TAMDAO	ME	3.056	4.179	1.872	1.870
		RMSE	3.130	4.318	2.152	2.149
	KIMBOI	ME	-2.627	-1.068	-0.248	-0.265
		RMSE	2.762	1.761	1.371	1.376

Note:
- ME: Mean error.
- RMSE: Root Mean Square Error.

3.2. Diurnal Temperature Cycle

This section evaluates the simulation of the diurnal cycle of temperature. Figure 4 compares the diurnal temperature cycle averaged for the JJA of 2000 and 2020 at stations in the Hanoi region, using 3-hourly RegCM5 outputs against ERA5 reanalysis, given the unavailability of sub-daily station data. Both datasets exhibit relatively similar diurnal patterns, with peak temperatures occurring between 10:00 and 13:00 LST. Consistent with the climatological results presented above, RegCM5 tends to produce higher temperatures than ERA5, and higher-resolution simulations generally yield warmer results, except at the TamDao station. Notably, differences are larger in 2020 than in 2000, particularly from the peak temperature period through midnight.

For highly urbanized stations, the differences between the default and updated urban cases are evident, particularly from late afternoon to late night (shaded columns in Fig. 4). These differences appear to be significantly influenced by changes in urbanization. In 2000, the updated urban case indicates a lower level of urbanization, resulting in negative differences. Conversely, in 2020, the differences are positive and considerably larger in magnitude. For non-urbanized stations, similar results are observed. In particular, at TamDao station, which is located at a relatively high elevation

(m), the CP 2 km experiments demonstrate their advantage in capturing detailed topography, leading to a significant reduction in temperature compared to ERA5 and the 10 km D1 simulations, mainly during daytime hours, and thus contributing to a reduced diurnal temperature range.

It is noteworthy that, compared to 2000, temperatures in 2020 are generally higher and exhibit a larger diurnal variation. For instance, at the Hanoi station, the CP-scale simulations indicate a diurnal temperature range of approximately 5°C in 2000 (with daily temperatures ranging from 28°C to 33°C). In contrast, the range increases to roughly 7°C in 2020 (with temperatures ranging from 29°C to 36°C). Similar results are observed at other highly urbanized stations. At non-urbanized stations, comparable patterns are recorded, though with smaller magnitudes.

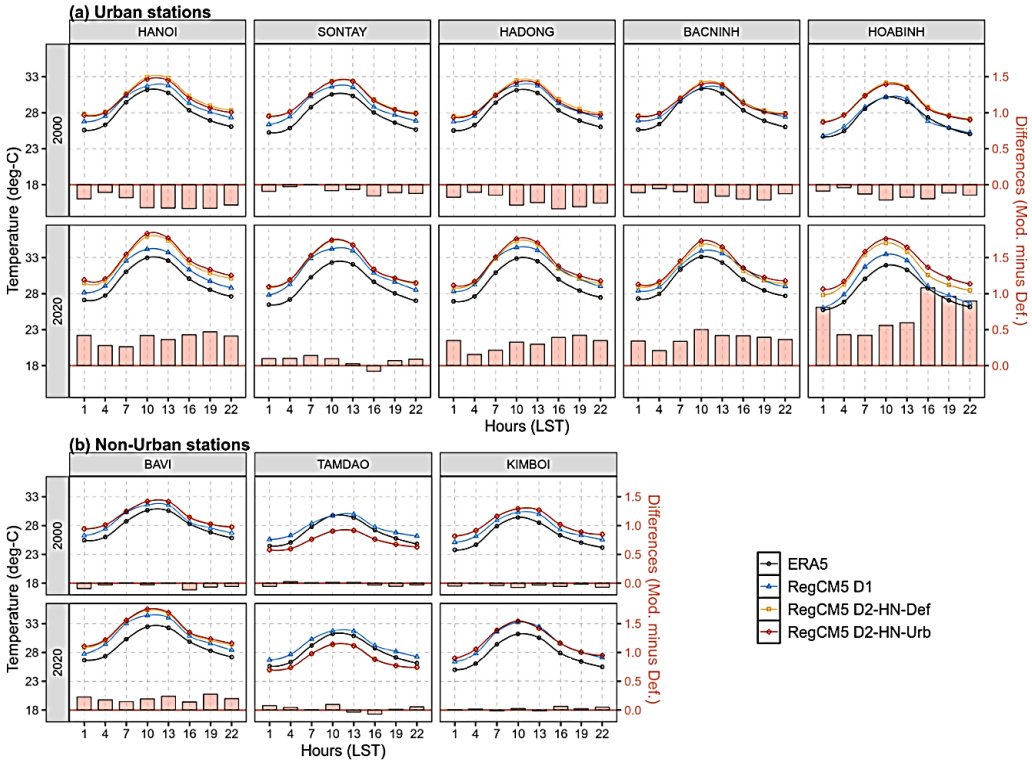

Figure 4. Comparison of the JJA diurnal cycle of 2-m temperature in 2000 and 2020 (lines, unit: °C) in the Hanoi domain, reproduced by ERA5 and the RegCM5 simulations for (a) highly urbanized stations, and (b) non-urbanized stations. The shaded columns represent the differences between the two CP-scale simulations at 2 km resolution (D2-HN-Urb minus D2-HN-Def). The left y-axis corresponds to line values, while the right y-axis corresponds to bar values.

To further validate the differences between the two CP-scale simulations and to examine model behaviors on a broader scale, Fig. 5 analyzes the diurnal cycle for both the Hanoi and Ho Chi Minh City domains. For this purpose, all grid points within each domain were divided into two categories: low-urbanized areas (urban fraction 0–15%) and high-urbanized areas (urban fraction. 15–100%). In contrast, completely non-urban grid points were excluded.

The results for 2000, 2005, 2015, and 2020 are consistent with previous analyses, showing that highly urbanized areas are

generally warmer, with higher peak temperatures and a clear warming trend toward the end of the study period. The differences between updated-urban minus default are more pronounced in highly urbanized areas, particularly from late afternoon through midnight. In both domains, these differences are slightly negative at the beginning of the period (2000) but become increasingly positive toward the end (2020), reflecting stronger warming under updated urban conditions. The magnitude of these differences is generally greater in Ho Chi Minh City than in Hanoi, suggesting more intense urbanization in the southern domain.

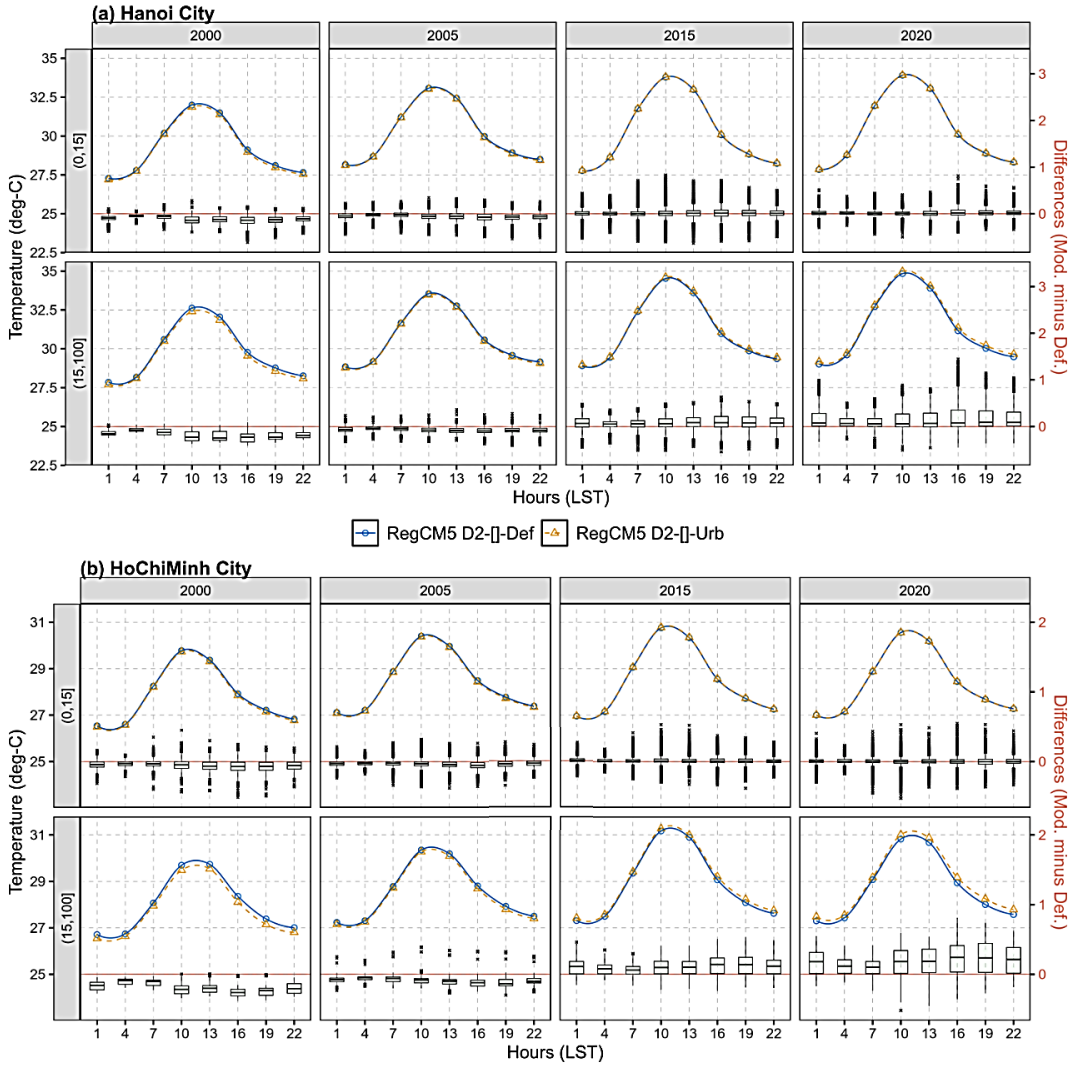

Figure 5. JJA diurnal cycle of 2-m temperature (lines, unit: °C) in 2000, 2005, 2015, and 2020 for (a) the Hanoi domain and (b) the Ho Chi Minh City domain, from D2 simulations using default and annually updated urban information. Lines represent averages for low-urbanized grid points (urban fraction < 15%, upper sub-panels) and highly urbanized grid points (urban fraction > 15%, lower sub-panels). Shaded bars indicate differences D2-HN-Urb minus D2-HN-Def. The left y-axis corresponds to line values, while the right y-axis corresponds to bar values.

3.3. Quantifying the UHI effect

Figure 6 illustrates the spatial distribution of the JJA average UHI effect across the two domains, Hanoi and Ho Chi Minh City, at different LSTs for the years 2000, 2010, and 2020. Both domains exhibit similar UHI patterns, with slightly higher magnitudes observed in Hanoi. From 2000 to 2020, as urbanization has expanded and intensified, the UHI effect has become more pronounced. The spatial distribution of UHI in Fig. 6 aligns with the population data presented in Fig. S1. Notably, both domains experience a strong UHI effect from 10:00 to 01:00 LST, peaking at 16:00 LST. This contrasts with the 2-m temperature results shown in Fig. S4, where hotter conditions are observed between approximately 7:00 and 16:00 LST. These findings reflect a common urban phenomenon in which heat is trapped within the urban canopy and released gradually until late at night, leading to prolonged thermal stress and limited nighttime recovery for urban residents after a hot day.

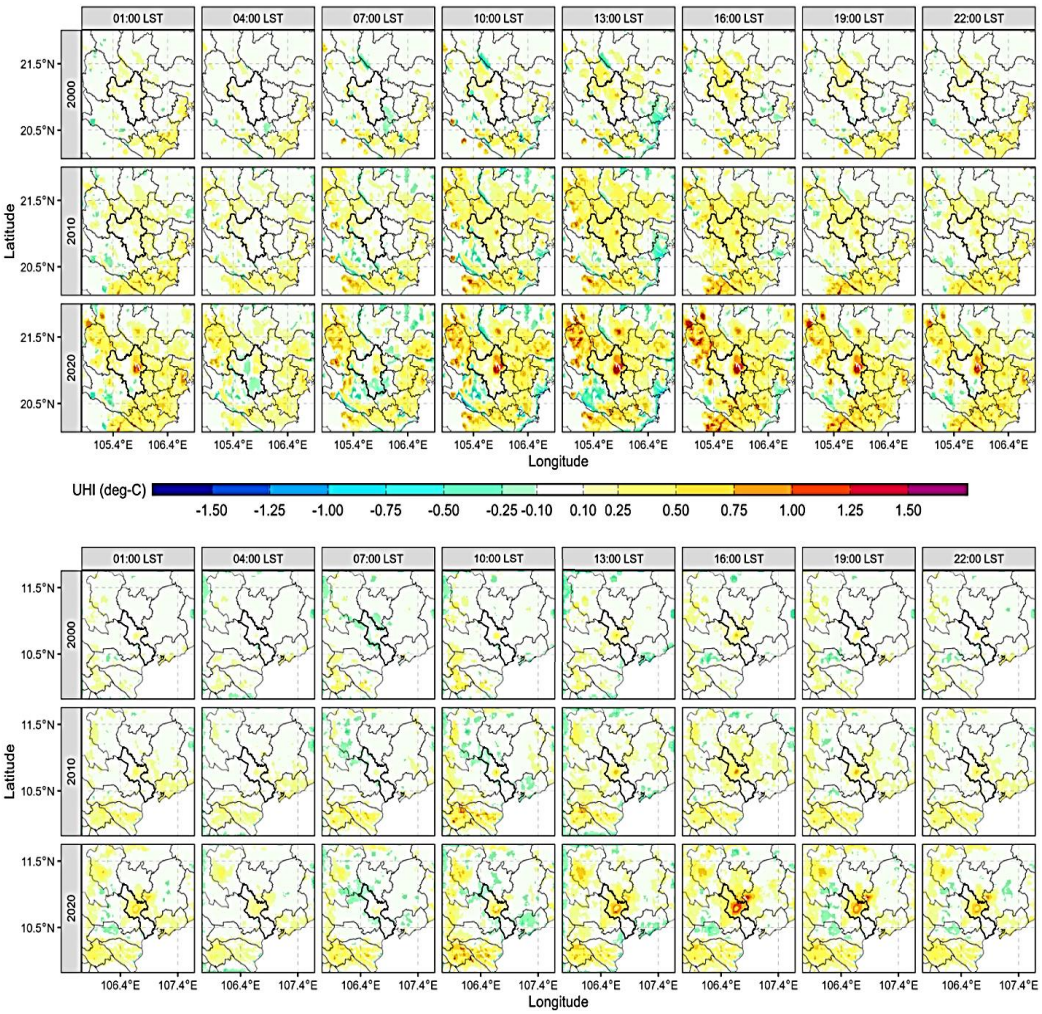

Figure 6. Spatial distribution of JJA average UHI effect (unit: °C) at different LST hours for the Hanoi (upper panels) and Ho Chi Minh City (lower panels) domains in 2000, 2010, and 2020

To examine whether a relationship exists between UHI intensity and background temperature, Fig. 7 explores the dependency of UHI on temperature anomaly. The analysis is conducted at a daily timescale at 10:00 LST when the temperature typically reaches a relatively high value, and at 16:00 LST when UHI intensity reaches its maximum. At each time, UHI intensity and temperature anomaly (relative to a 21-year climatology) are first computed at individual grid points and then area-averaged for each domain. As shown in Fig. 7, the Hanoi domain exhibits an apparent increase in UHI intensity, with a stronger correlation with background temperature toward the end of the study period. A similar, though weaker, signal is recorded in the Ho Chi Minh City domain, primarily due to the area-averaging process, which may smooth out the signal since urban development is concentrated mainly around the city center.

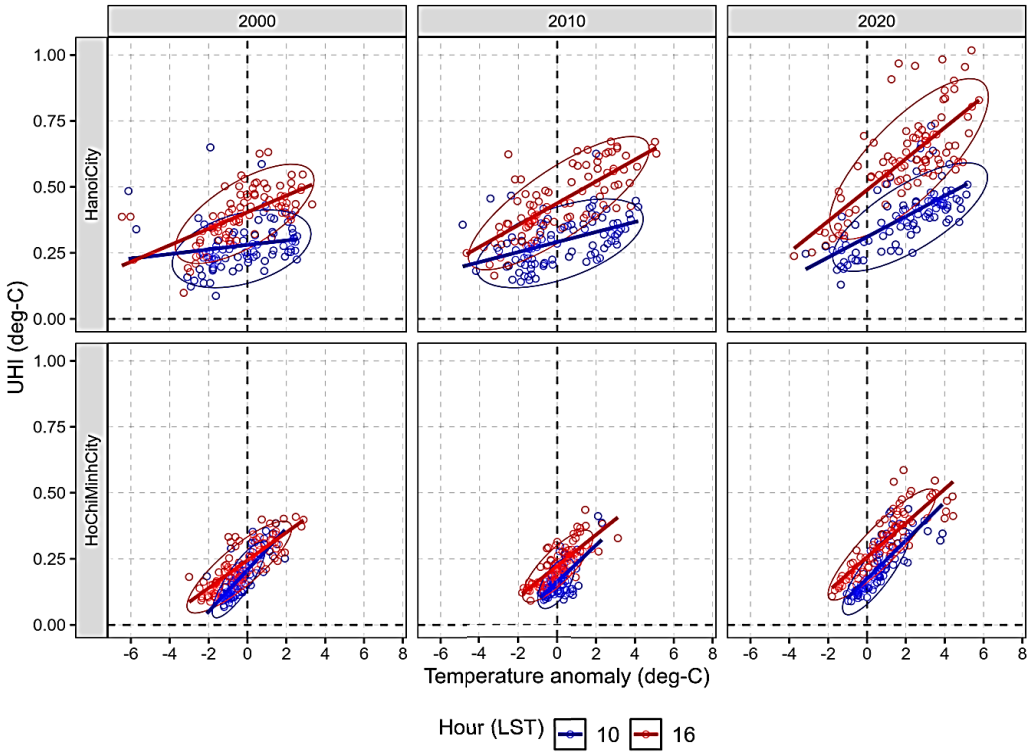

Figure 7. Dependency of UHI on temperature anomaly for the years 2000, 2010, and 2020 (left to right), area-averaged for the Hanoi (upper panels) and Ho Chi Minh City (lower panels) domains at 10:00 LST (blue) and 16:00 LST (red). In each panel, the ellipse represents the 99% confidence region based on a multivariate t-distribution, while the line indicates a simple linear regression with UHI intensity as a function of the near-surface temperature anomaly.

The findings suggest that the intensity of the UHI effect is more pronounced on exceptionally hot days. Consequently, on abnormally hot summer days, the potential for severe heat stress increases significantly in urban areas. Notably, the UHI values depicted in Fig. 7 are area-averaged across the entire domain, indicating that certain urban regions may experience UHI intensities that far exceed the area-averaged values. These localized temperature increases due to the UHI effect further exacerbate heat-related

risks, especially for urban residents living in vulnerable or poorly conditioned environments.

4. Conclusions

This study demonstrates the potential of using RegCM5 for downscaling to a convection-permitting scale in Vietnam, with a focus on the long-term effects of urbanization in Hanoi and Ho Chi Minh City. Simulations were first conducted at a 10 km resolution and subsequently downscaled to 2 km, both with and without annual updates to urban data. The results were evaluated against the well-known ERA5 reanalysis, the VnGC gridded dataset, and station observations.

Our analysis showed that the RegCM5 model with the new MOLOCH dynamic core performs well at CP-scale resolutions, offering stable operation and faster performance compared to earlier versions. The 2 km simulations often outperform both ERA5 and VnGC when compared with station data, highlighting the need for higher-quality and higher-resolution gridded observational products. We further examined the effects of urbanization on regional climate in Hanoi and Ho Chi Minh City. The results indicate that urbanization has a substantial impact on local climate conditions. The simulations incorporating annually updated urban data show elevated temperatures towards the end of the study period, especially from late afternoon to late night. Urbanization also intensifies the Urban Heat Island (UHI) effect, most notably between 10:00 and 01:00 LST. Additionally, a strong correlation is observed between UHI intensity and background temperature, implying a potential link between urban effects and broader climate change. For instance, rapid urbanization will amplify the adverse impacts of global warming on local communities.

In this study, we acknowledge several limitations that could not be fully addressed. First, the RegCM5 configuration employed was adapted from a previous setup optimized for precipitation simulations at a 10 km resolution. Second, we incorporated annual urban changes solely based on population data, which may not accurately represent actual urban development and land surface characteristics within each study domain, potentially introducing biases in model results. Third, our analysis is limited to temperature-related effects, whereas urbanization can influence other meteorological variables such as humidity, wind speed, and radiation. The model's ability to simulate these variables is crucial, particularly when used as inputs for further impact studies (Qian et al., 2022). Fourth, in all our analyses comparing the two domains, both temperature and UHI intensity values consistently appear higher in Hanoi than in Ho Chi Minh City. This does not imply that the climatic conditions in Ho Chi Minh City are less severe. Due to time and computational constraints, the downscaling simulations were derived from a parent domain covering only May-August. As a result, our analysis for Ho Chi Minh City is limited to JJA, which represents the hottest months in Hanoi but not in the south. This limitation should be addressed in future research.

Last but not least, the results of our study offer valuable insights for future research, which are not only relevant to Vietnam but also contribute meaningfully to the modeling community, particularly those working with RegCM5. While there is room for further refinement, the modeling framework and results presented here demonstrate substantial potential to support policy development. and decision-making processes. This is particularly timely as Vietnam moves to update its national climate change and sea level rise scenarios, where high-resolution climate simulations and detailed urban climate analyses are in high demand to enable robust, evidence-based planning and risk assessment.

Acknowledgements

This work is supported by the Vietnam Academy of Science and Technology (VAST) grant number THTETN.03/23-24.

References

Coppola E., Stocchi P., Pichelli E., Torres Alavez J.A., Glazer R., Giuliani G., Di Sante F., Nogherotto R., Giorgi F., 2021. Non-Hydrostatic RegCM4 (RegCM4-NH): model description and case studies over multiple domains. Geosci. Model Dev., 14, 7705–7723. https://doi.org/10.5194/gmd-14-7705-2021.

Davolio S., Malguzzi P., Drofa O., Mastrangelo D., Buzzi A., 2020. The Piedmont flood of November 1994: a testbed of forecasting capabilities of the CNR-ISAC meteorological model suite. Bull. of Atmos. Sci. & Technol., 1, 263–282. https://doi.org/10.1007/s42865-020-00015-4.

Emanuel K.A., 1991. A Scheme for Representing Cumulus Convection in Large-Scale Models. J. Atmos. Sci., 48, 2313–2329. https://doi.org/10.1175/1520-0469(1991)048<2313:ASFRCC>2.0.CO;2.

Gao J., O'Neill B.C., 2020. Mapping global urban land for the 21st century with data-driven simulations and Shared Socioeconomic Pathways. Nat Commun, 11, 2302. https://doi.org/10.1038/s41467-020-15788-7.

Giorgi, F., 1990. Simulation of Regional Climate Using a Limited Area Model Nested in a General Circulation Model. J. Climate, 3, 941–963. https://doi.org/10.1175/1520-0442(1990)003<0941:SORCUA>2.0.CO;2.

Giorgi F., 2019. Thirty Years of Regional Climate Modeling: Where Are We and Where Are We Going next? JGR Atmospheres, 124, 5696–5723. https://doi.org/10.1029/2018JD030094.

Giorgi F., Coppola E., Giuliani G., Ciarlo' J.M., Pichelli E., Nogherotto R., Raffaele F., Malguzzi P., Davolio S., Stocchi P., Drofa O., 2023. The Fifth Generation Regional Climate Modeling System, RegCM5: Description and Illustrative Examples at Parameterized Convection and Convection-Permitting Resolutions. JGR Atmospheres 128, e2022JD038199. https://doi.org/10.1029/2022JD038199.

Grimmond C.S.B., et al., 2009. Urban surface energy balance models: model characteristics and methodology for a comparison study. In: Baklanov, A., et al. (Eds.), Meteorological and Air Quality Models for Urban Areas. https://doi.org/10.1007/978-3-642-00298-4_11.

Hersbach H., Bell B., Berrisford P., Hirahara S., Horányi A., Muñoz-Sabater J., Nicolas J., Peubey C., Radu R., Schepers D., Simmons A., Soci C., Abdalla S., Abellan X., Balsamo G., Bechtold P., Biavati G., Bidlot J., Bonavita M., De Chiara G., Dahlgren P., Dee D., Diamantakis M., Dragani R., Flemming J., Forbes R., Fuentes M., Geer A., Haimberger L., Healy S., Hogan R.J., Hólm E., Janisková M., Keeley S., Laloyaux P., Lopez P., Lupu C., Radnoti G., De Rosnay P., Rozum I., Vamborg F., Villaume S., Thépaut J., 2020. The ERA5 global reanalysis. Quart J Royal Meteoro Soc., 146, 1999–2049. https://doi.org/10.1002/qj.3803.

Hoang-Cong H., Ngo-Duc T., Nguyen-Thi T., Trinh-Tuan L., Jing Xiang C., Tangang F., Jerasorn S., Phan-Van T., 2022. A high-resolution climate experiment over part of Vietnam and the Lower Mekong Basin: performance evaluation and projection for rainfall. Vietnam Journal of Earth Sciences, 44(1), 92–108. https://doi.org/10.15625/2615-9783/16942.

Holtslag A.A.M., De Bruijn E.I.F., Pan H.-L., 1990. A High Resolution Air Mass Transformation Model for Short-Range Weather Forecasting. Mon. Wea. Rev., 118, 1561–1575. https://doi.org/10.1175/1520-0493(1990)118<1561:AHRAMT>2.0.CO;2.

Jackson T.L., Feddema J.J., Oleson K.W., Bonan G.B., Bauer J.T., 2010. Parameterization of Urban Characteristics for Global Climate Modeling. Annals of the Association of American Geographers, 100, 848–865. https://doi.org/10.1080/00045608.2010.497328.

Kiehl J., Hack J., Bonan G., Boville B., Williamson D., Rasch P., 1998. The national center for atmospheric research community climate model: CCM3. J. Climate, 11, 1131–1149.

Lowry W.P., 1977. Empirical Estimation of Urban Effects on Climate: A Problem Analysis. J. Appl. Meteor., 16, 129–135. https://doi.org/10.1175/1520-0450(1977)016<0129:EEOUEO>2.0.CO;2.

Martin-Vide J., Sarricolea P., Moreno-GarcÃ-a M.C., 2015. On the definition of urban heat island intensity: the "rural" reference. Front. Earth Sci., 3. https://doi.org/10.3389/feart.2015.00024.

Ngo-Duc T., Nguyen-Duy T., Desmet Q., Trinh-Tuan L., Ramu L., Cruz F., Dado J.M., Chung J.X., Phan-Van T., Pham-Thanh H., Truong-Ba K., Tangang F.T., Juneng L., Santisirisomboon J., Srisawadwong R., Permana D., Linarka U.A., Gunawan D., 2024. Performance Ranking of Multiple CORDEX-SEA Sensitivity Experiments: Towards an Optimum Choice of Physical Schemes for RegCM over Southeast Asia. Climate Dynamics, 62, 8659–8673. https://doi.org/10.1007/s00382-024-07353-5.

Nguyen-Le D., Trinh-Tuan L., Nguyen-Xuan T., Nguyen-Duy T., Ngo-Duc T., 2025. Projections of Heat Stress in Vietnam Using Physically-Based Wet-Bulb Globe Temperature. AFD Research papers, 346, 50. https://www.afd.fr/en/ressources/projections-heat-stress-vietnam-using-physically-based-wet-bulb-globe-temperature.

Nguyen-Ngoc-Bich P., et al., 2022. Projected future changes in drought characteristics over Southeast Asia. Vietnam Journal of Earth Sciences, 44(1), 127–143. https://doi.org/10.15625/2615-9783/16974.

Nguyen-Thi T., Ngo-Duc T., Phan-Van T., 2019. Performance of SEACLID/CORDEX-SEA multi-model experiments in simulating temperature and rainfall in Vietnam. Vietnam Journal of Earth Sciences, 41(4), 374–387. https://doi.org/10.15625/0866-7187/41/4/14259.

Nguyen-Xuan T., Im E.-S., 2023. Assessing the performance of the non-hydrostatic RegCM4 with the improved urban parameterization over southeastern China. Urban Climate, 49, 101527. https://doi.org/10.1016/j.uclim.2023.101527.

Nguyen-Xuan T., Zhou Z., Nguyen-Duy T., Nguyen-Le D., Ngo-Duc T., 2025. Optimizing Configurations for the Regional Climate Model (RegCM5) Using a Micro-GA Approach: A Case Study over Vietnam. Scientific Online Letters on the Atmosphere (SOLA), 21, 391–395. https://doi.org/10.2151/sola.2025-053.

Nogherotto R., Tompkins A.M., Giuliani G., Coppola E., Giorgi F., 2016. Numerical framework and performance of the new multiple-phase cloud microphysics scheme in RegCM4.5: precipitation, cloud microphysics, and cloud radiative effects. Geosci. Model Dev., 9, 2533–2547. https://doi.org/10.5194/gmd-9-2533-2016.

Oleson K.W., Feddema J., 2020. Parameterization and Surface Data Improvements and New Capabilities for the Community Land Model Urban (CLMU). J Adv Model Earth Syst, 12, e2018MS001586. https://doi.org/10.1029/2018MS001586.

Oleson K.W., Lawrence D.M., 2013. Technical description of version 4.5 of the community land model (CLM). NCAR Technical Note NCAR/TN-503+STR, NCAR, Boulder, CO, USA.

Open Topography, 2013. Shuttle Radar Topography Mission (SRTM) Global. https://doi.org/10.5069/G9445JDF.

Pal J.S., Giorgi F., Bi X., Elguindi N., Solmon F., Gao X., Rauscher S.A., Francisco R., Zakey A., Winter J., Ashfaq M., Syed F.S., Bell J.L., Diffenbaugh N.S., Karmacharya J., Konaré A., Martinez D., Da Rocha R.P., Sloan L.C., Steiner A.L., 2007. Regional Climate Modeling for the Developing World: The ICTP RegCM3 and RegCNET. Bulletin of the American Meteorological Society, 88, 1395–1410. https://doi.org/10.1175/BAMS-88-9-1395.

Pal J.S., Small E.E., Eltahir E.A.B., 2000. Simulation of regional-scale water and energy budgets: Representation of subgrid cloud and precipitation processes within RegCM. J. Geophys. Res., 105, 29579–29594. https://doi.org/10.1029/2000JD900415.

Qian Y., Chakraborty T.C., Li J., Li D., He C., Sarangi C., Chen F., Yang X., Leung L.R., 2022. Urbanization impact on regional climate and extreme weather: current understanding, uncertainties, and future research directions. Adv. Atmos. Sci., 39, 819–860. https://doi.org/10.1007/s00376-021-1371-9.

Shepard D., 1968. A two-dimensional interpolation function for irregularly-spaced data, in: Proceedings of the 1968 23rd ACM National Conference. ACM Press, 517–524. https://doi.org/10.1145/800186.810616.

Tiedtke M., 1989. A Comprehensive Mass Flux Scheme for Cumulus Parameterization in Large-Scale Models. Mon. Wea. Rev., 117, 1779–1800. https://doi.org/10.1175/1520-0493(1989)117<1779:ACMFSF>2.0.CO;2.

Trinh-Tuan L., Ngo-Duc T., Phan-Van T., 2019. Vietnam Gridded Climate Dataset Version 2: Preliminary Results, In: Proceeding of the Carees 2019 workshop on Basic Research in the Field of Earth and Environmental Sciences. Publishing House for Science and Technology, Hanoi, Vietnam. https://doi.org/10.15625/vap.2019.000147.

Ünal Y.S., Sonuç C.Y., Incecik S., Topcu H.S., Diren-Üstün D.H., Temizöz H.P., 2020. Investigating urban heat island intensity in Istanbul. Theor Appl Climatol, 139, 175–190. https://doi.org/10.1007/s00704-019-02953-2.

United Nations, Department of Economic and Social Affairs, 2018. World Urbanization Prospects: The 2018. Revision, 123p. https://doi.org/10.18356/b9e995fe-en.

Yan Z.-W., Wang J., Xia J.-J., Feng J.-M., 2016. Review of recent studies of the climatic effects of urbanization in China. Advances in Climate Change Research, 7, 154–168. https://doi.org/10.1016/j.accre.2016.09.003.

Zeng X., Zhao M., Dickinson R.E., 1998. Intercomparison of bulk aerodynamic algorithms for the computation of sea surface fluxes using TOGA COARE and TAO data. J Clim, 11(10), 2628–2644. https://doi.org/10.1175/1520-0442(1998)011%3c2628:IOBAAF%3e2.0.CO;2.

SUPPLEMENTARY MATERIALS

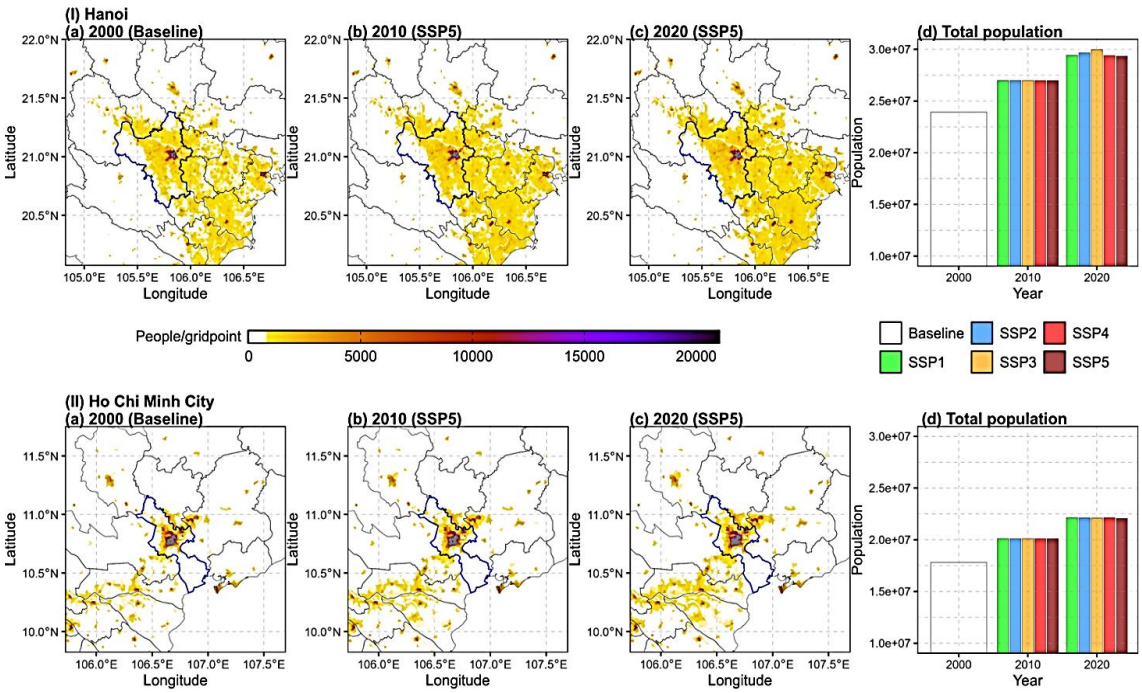

Figure S1. Spatial distribution of the population (unit: people per km²) in the (I) Hanoi and (II) Ho Chi Minh City domains for the years (a) 2000, (b) 2010, and (c) 2020. Panel (d) for each domain shows the total population for the base year 2000, as well as for the years 2010 and 2020 under the five SSP scenarios

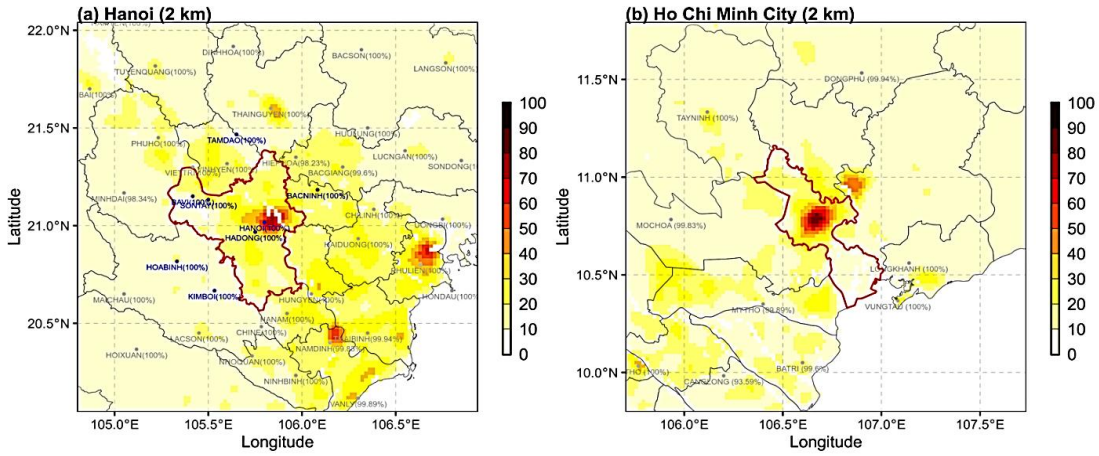

Figure S2. Locations of meteorological stations in the (a) Hanoi and (b) Ho Chi Minh City domains. The number in brackets next to each station name indicates the percentage of available days during JJA for the period 2000–2020

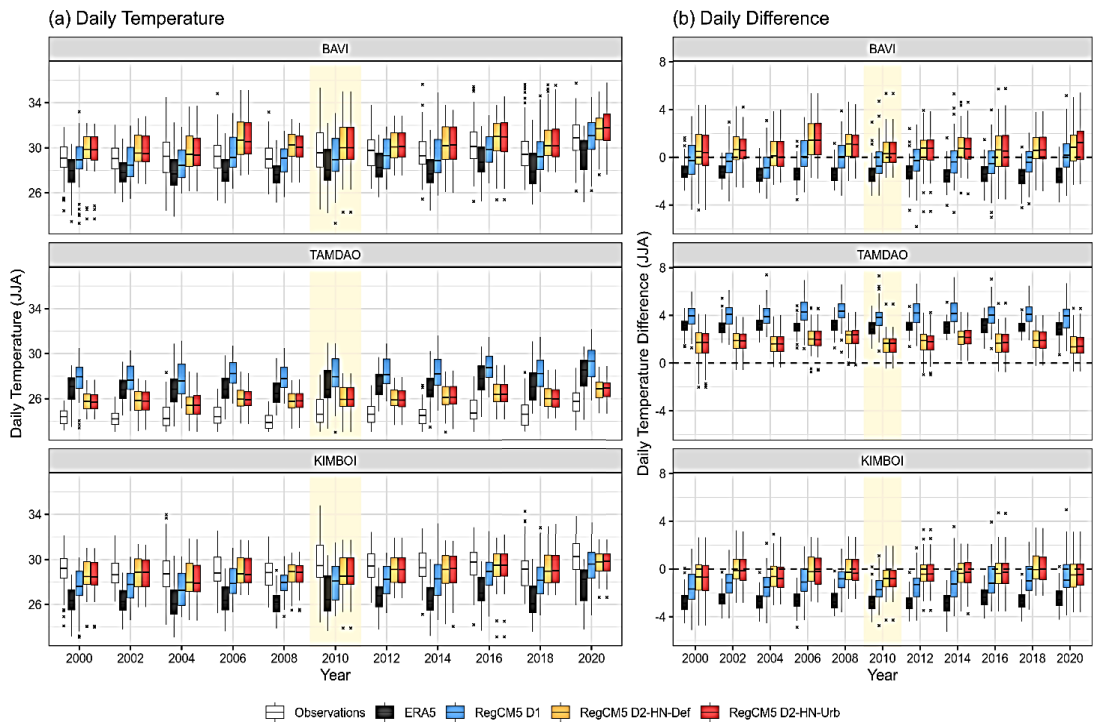

Figure S3. Boxplot at specific non-urbanized stations in the Hanoi domain for yearly comparison of: (a) daily 2-m temperature (unit: °C) observed by station measurements and reproduced by ERA5, the D1 experiment at 10 km resolution, and the D2-HN-Def and D2-HN-Urb experiments at 2 km resolution; (b) daily differences (unit: °C) between the model products and station observations. The year 2010 is highlighted with yellow shading to indicate that both D2 simulations share the same urban information for this year

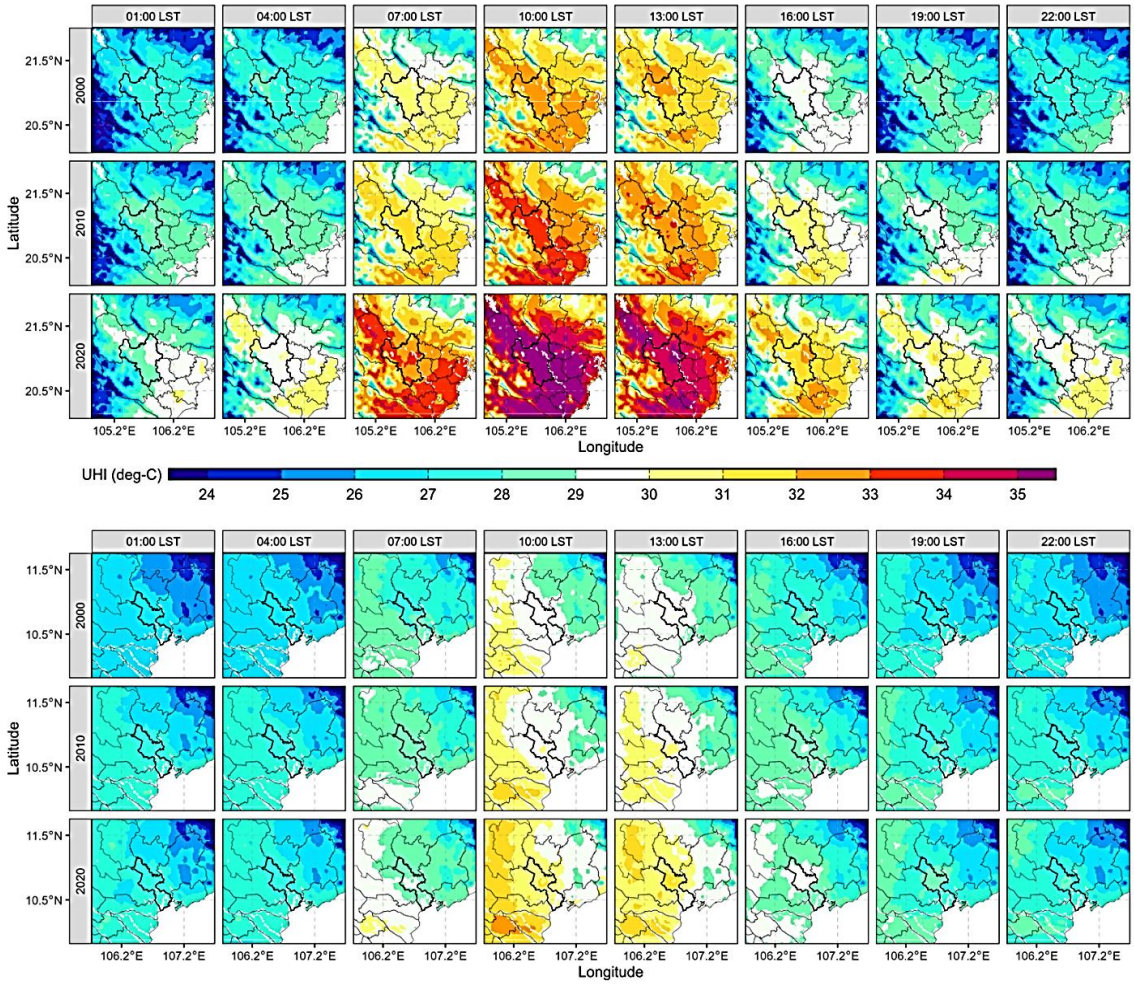

Figure S4. Spatial distribution of JJA average 2m-temperature (unit: °C) at different LST hours for the Hanoi (upper panels) and Ho Chi Minh City (lower panels) domains in 2000, 2010, and 2020